Annexin V Binds to Viable B Cells and Colocalizes with a Marker of Lipid Rafts upon B Cell Receptor Activation[1]

Stacey R. Dillon,[2] Marie Mancini, Antony Rosen, and Mark S. Schlissel[3]

Recombinant annexin V (rAnV) has been used to identify apoptotic cells based on its ability to bind phosphatidylserine (PS), a lipid normally restricted to the cytoplasmic face of the plasma membrane, but externalized early during apoptosis. However, this association of rAnV binding and apoptosis is not an obligatory one. We demonstrate that rAnV binds to a large fraction of murine B cells bearing selectable Ag receptors despite the fact that these cells are not apoptotic. Phosphatidylserine, which is uniformly distributed on resting B cells, is mobilized to co-cap with IgM on anti-IgM-treated B cells and to colocalize with GM1, a marker of lipid rafts. Cross-linking PS before anti-IgM treatment sequesters this lipid and alters signaling through IgM. Thus, PS exposed on the majority of B cells in vivo does not reflect early apoptosis, but, instead, plays a role in receptor-mediated signaling events. *The Journal of Immunology,* **2000, 164: 1322–1332.**

B cells undergo selection at multiple stages during their development based largely on their ability to express a functional and self-tolerant B cell receptor (BCR)[4] for Ag (reviewed in Ref. 1). The genes encoding this receptor, Ig heavy (IgH) and light (IgL) chain genes, are assembled by V(D)J recombination in a highly regulated fashion during the early stages of B cell development (reviewed in Ref. 2). Unsuccessful rearrangement of Ig genes results in the apoptosis of developing B cells (3). After successful gene rearrangement, nascent, immature B cells express sIgM, but not sIgD, while mature B cells express both sIgM and sIgD. There are two subsets of peripheral B cells, called B-2 and B-1 (reviewed in Ref. 4). These subsets express distinct Ig repertoires, presumably reflecting their different functions in the immune system (5). The B-2 cell Ig repertoire is exceptionally diverse, while the B-1 cell repertoire is more limited. B-2 cells predominate in the blood, spleen, and lymph nodes and participate in T cell-dependent immune responses. B-1 cells are largely restricted to the peritoneum and other body cavities and comprise the majority of B cells in these areas. B-1 cells have the capacity for self-renewal and are responsible for secreting most of the IgM present in the serum of unimmunized animals (6). Because a large fraction of the B-1 subset is composed of cells with measurable affinity for self Ags with repetitive structures, such as phosphatidylcholine (PC) and DNA (7–9), it has been suggested that developing B cells bearing certain self-specific Ag receptors are positively selected into the B-1 cell repertoire (10).

Transgenic (Tg) mouse model systems have clearly demonstrated that B cells that generate a BCR capable of recognizing self Ag with high affinity may edit that receptor by replacing the IgH and/or IgL chain gene segments through further V(D)J recombination (11–13). Self-reactive immature B cells that fail to edit their receptors successfully are negatively selected at an immature stage of development (14, 15) and die by apoptosis in situ, analogous to thymocytes expressing an autoreactive TCR (16, 17). B cells that survive this stringent selection process are exported to the peripheral lymphoid organs to participate in immune surveillance.

The plasma membrane of a healthy cell typically exhibits an asymmetric distribution of its major phospholipids, maintained by the activity of aminophospholipid translocase (18). Virtually all of the phosphatidylserine (PS) and most of the phosphatidylethanolamine (PtE) and phosphatidylinositol (PI) molecules reside on the inner leaflet of the plasma membrane, with sphingomyelin (SM) largely confined to the outer leaflet, and PC distributed equally between the leaflets (19). During the early stages of apoptosis, cells lose their membrane phospholipid asymmetry and expose PS on the outer leaflet of the plasma membrane, triggering their phagocytosis by macrophages that bear PS receptors (20). Rapid phagocytosis prevents secondary necrosis and inflammation within the surrounding tissue (reviewed in Refs. 21 and 22).

Annexin V (AnV) is a member of a large family of Ca^{2+} and phospholipid binding proteins (23). In the presence of physiological concentrations of Ca^{2+}, AnV has high affinity for negatively charged phospholipids, especially PS. Based on its affinity for PS, fluorescently labeled AnV is often used in flow cytometric assays to detect cells undergoing apoptosis (24, 25). The original intent of the studies described below was to use recombinant AnV (rAnV) to study apoptosis at various stages during murine B cell development. Contrary to our expectations, we found that rAnV binds to the outer leaflet of the plasma membrane in healthy B cells, associates with the BCR in membrane microdomains in anti-IgM-activated B cells, and affects the signaling activity of the BCR on splenic B cells.

Departments of Medicine, Molecular Biology and Genetics, and Oncology, Division of Rheumatology, Johns Hopkins University School of Medicine, Baltimore, MD 21205

Received for publication September 8, 1999. Accepted for publication November 10, 1999.

The costs of publication of this article were defrayed in part by the payment of page charges. This article must therefore be hereby marked *advertisement* in accordance with 18 U.S.C. Section 1734 solely to indicate this fact.

[1] This work was supported in part by U.S. Public Health Service Grant HL48722 (to M.S.S.) and a Biomedical Science Research Grant from the Arthritis Foundation (to M.S.S.). S.R.D. was a recipient of an Arthritis Foundation Postdoctoral Fellowship, A.R. is a Pew Scholar in the Biomedical Sciences, and M.S.S. acknowledges the support of a Leukemia Society Scholarship.

[2] Current address: ZymoGenetics, 1201 Eastlake Avenue East, Seattle, WA 98102.

[3] Address correspondence and reprint requests to Dr. Mark Schlissel at the current address: Department of Molecular and Cell Biology, 439 LSA, University of California, Berkeley, CA 94720-3200. E-mail address: mss@uclink4.berkeley.edu

[4] Abbreviations used in this paper: BCR, B cell receptor; BM, bone marrow; CTx, cholera toxin; MC540, merocyanine 540; $\Delta\psi_m$, mitochondrial transmembrane potential; PARP, poly(A)DP-ribose polymerase; PC, phosphatidylcholine; PI, phosphatidylinositol; PS, phosphatidylserine; PtE, phosphatidylethanolamine; QR, Quantum Red; rAnV, recombinant annexin V; SA, streptavidin; 7AAD, 7-amino-actinomycin D; (s)HEL, (soluble) hen egg lysozyme; SM, sphingomyelin; Tg, transgenic; β_2m, β_2-macroglobulin; WB, wash buffer.

0022-1767/00/$02.00

Materials and Methods

Mice

The Tg mice expressing the Ig H+L chain genes from the 3-83 BCR that confers reactivity to the mouse MHC class I Ags H-2K^b and -K^k (26) were provided by Dr. David Scott (American Red Cross, Rockville, MD) and maintained on an H-2^d background by continuous backcrosses to BALB/c mice (National Cancer Institute, Frederick, MD). 3-83 Tg mice were also bred to H-2^b β_2m$^{-/-}$ mice (27), which were the gift of Dr. Mark Soloski (Johns Hopkins University). Mice expressing Ig H+L transgenes encoding a BCR specific for HEL and anti-HEL/soluble HEL double Tg mice (28) were obtained from Dr. Tim Behrens (University of Minnesota, Minneapolis, MN) or from The Jackson Laboratory (Bar Harbor, ME). V_H12 Tg mice (29), which carry a rearranged Ig H chain gene from a PC-specific B-1a clone, were provided by Dr. Stephen Clarke (University of North Carolina, Chapel Hill). Both anti-HEL Tg and V_H12 Tg mice were maintained as heterozygotes by continuous backcrosses to C57BL/6 mice. Control non-Tg mice were offspring from these same matings. Mice were maintained in specific pathogen-free conditions in our facility and unless otherwise noted were used in experiments at 4–20 wk of age.

Reagents

Recombinant human AnV was cloned by PCR, expressed in *Escherichia coli*, then purified and conjugated to FITC or biotin as previously described (30). Our reagent gave results identical with those using commercially prepared versions of FITC-rAnV (Clontech, Palo Alto, CA) or biotin-rAnV (PharMingen, San Diego, CA). TUNEL assays were performed with a kit (Roche, Indianapolis, IN) according to the manufacturer's instructions. 4′,6-Diamidino-2-phenylindole and DiOC$_6$ were obtained from Molecular Probes (Eugene, OR); 7AAD, MC540, Quantum Red (QR)-SA, and FITC-cholera toxin (CTx; β subunit) were purchased from Sigma (St. Louis, MO). Unlabeled SA used in cross-linking experiments was purchased from ICN (Irvine, CA). Anti-B220-PE (clone RA3-6B2), anti-CD3ϵ-biotin (clone 2C11), and anti-CD19-biotin (clone 1D3) mAbs were obtained from PharMingen. Unlabeled and PE-labeled goat anti-mouse IgM, PE-goat anti-mouse IgG2a, and goat anti-mouse IgD-biotin were purchased from Southern Biotechnology Associates (Birmingham, AL). Both FITC- and biotin-conjugated versions of 54.1, the mAb that recognizes the 3-83 Id, were gifts from Terri Grdina (American Red Cross). The anti-mouse MHC class I (H-2K^b, L^d) mAb 28-14-8, a mouse IgG2a mAb, was provided by Dr. Mark Soloski (Johns Hopkins University, Baltimore, MD). The mouse anti-α-fodrin mAb 1622 was purchased from Chemicon International (Temecula, CA), and HRP-conjugated sheep anti-mouse Ig was purchased from Amersham (Arlington Heights, IL). 4G10, a mouse anti-phosphotyrosine mAb, was obtained from Upstate Biotechnology (Lake Placid, NY). 60.815 is a human anti-human poly(A)DP-ribose polymerase (PARP) antisera that cross-reacts on mouse PARP (31); HRP-conjugated goat anti-human Ig was purchased from Southern Biotechnology Associates.

Apoptosis control cell line

103-bcl2 cells (32) were obtained from Dr. Naomi Rosenberg (Tufts University, Boston, MA) and were grown in RPMI 1640 supplemented with 10% FBS, 4 mM glutamine, 10 mM HEPES, 50 μM 2-ME, and antibiotics at 33°C in a 5% CO_2 incubator. For induction of apoptosis, the cells were shifted to 39°C for 12–16 h.

Cell preparation and purification

BM cells were isolated from femurs and tibias by careful disruption in PBS using a mortar and pestle. Cells were resuspended, depleted of bone fragments by passive sedimentation, and pelleted at 1000 × *g*. Splenocytes were obtained by crushing spleens between glass slides, then resuspending and pelleting the cells as described for BM. To avoid the potential loss or gain of rAnV$^+$ cells, BM and spleen samples were not depleted of RBC by Ficoll treatment or hypotonic lysis; instead, RBC and dead cells were gated out electronically after flow cytometric analysis. All cells were resuspended in FACS wash buffer (FACS WB; HBSS, 1% BSA, and 10 mM HEPES, pH 7.4) at a concentration of 20–30 × 10^6 c/ml before staining. To enrich for B cells, BM or spleen preparations were stained with anti-CD19-biotin followed by a wash by SA-conjugated magnetic beads, then passed over a MiniMacs separation column according to the manufacturer's instructions (Miltenyi Biotec, Sunnyvale, CA).

Pronase digestion of splenocytes

Splenocytes were purified by Ficoll-gradient centrifugation and resuspended in HBSS and 10 mM HEPES, pH 7.5, before incubation for 5 min at 37°C in the presence or the absence of 50 μg/ml pronase (Roche). Cells were transferred to an ice bucket, and an excess of ice-cold HBSS and 10% newborn calf serum was added. Cells were then recovered by centrifugation and washed two additional times in HBSS and 10% newborn calf serum. Finally, cells were resuspended in FACS WB and analyzed by flow cytometry as described below.

Cell staining and flow cytometry

For staining with FITC- or biotin-rAnV, 1–1.5 × 10^6 cells were transferred to 5-ml tubes and washed with 1 ml of FACS WB and 2 mM $CaCl_2$ or WB and 2 mM EGTA, then pelleted at 1000 × *g*. The interaction between AnV and PS is calcium dependent and as such should be abolished in the presence of EGTA. Cells were then incubated on ice for 20 min in the presence of saturating amounts of the appropriate FITC-, PE-, and/or biotin-conjugated mAbs and FITC- or biotin-rAnV in a total volume of 100 μl of FACS WB with Ca^{2+} or EGTA. Cells were washed with 1.5 ml of WB and Ca^{2+} or EGTA, pelleted, then resuspended in 100 μl WB and Ca^{2+} or EGTA containing a saturating amount of QR-SA. After another 20-min incubation on ice, the cells were washed and pelleted as before, then resuspended in 0.5 ml of WB and Ca^{2+} or EGTA and analyzed on a FACScan using CellQuest software (Becton Dickinson, Mountain View, CA), except for those analyses shown in Fig. 3*B*, which were performed on a Coulter EPICS-EL cytometer (Coulter, Hialeah, FL) and analyzed with FloJo software (Tree Star, San Carlos, CA). MC540 was added just before FACS analysis at a final concentration of 0.1 μg/ml. Cells were stained with DiOC$_6$ (40 nM, final concentration) for 15 min at 37°C and were washed before staining with other reagents. Detectors for forward and side light scatter were set on a linear scale, whereas logarithmic detectors were used for all three fluorescence channels (FL-1, FL-2, and FL-3). Compensation for spectral overlap between FL channels was performed for each experiment using single-color-stained cell populations. Wherever possible, instrument settings were saved to disk and used again with slight modifications if necessary in related experiments. All cells were collected ungated to disk, and data were analyzed using CellQuest software. Unless otherwise noted, RBC and dead cells were excluded by electronically gating data on the basis of FSC vs SSC profiles; a minimum of 10^4 cells of interest were analyzed further.

Liposome inhibition of rAnV binding

Liposomes, generated essentially as previously described (33), were composed of 70% PC and 30% of each of the phospholipids PS, PI, phosphatidic acid, SM, and PtE, or 100% PC. Pure preparations of lipids (Sigma) were added to glass tubes in appropriate combinations, mixed gently, evaporated to dryness under N_2 gas, resuspended in HEPES buffer to a final concentration of 1 mM, then sonicated on ice for 5 min. Liposomes were used within 2 h of preparation. Before staining cells with FITC-AnV, liposomes were added to the FITC-rAnV solution at a predetermined optimal concentration (5 μM), followed by incubation for 10 min at room temperature. Cells were stained with the AnV/liposome mixture in the usual manner, washed thoroughly, stained with B220-PE followed by 7AAD, and then analyzed on a FACScan.

Western immunoblotting

To analyze the status of α-fodrin cleavage in various cell populations, cells were washed twice with PBS, pelleted, and resuspended in an equal volume of PBS and 2× SDS gel loading buffer (17% glycerol, 5% SDS, 0.05% bromophenol blue, 1.4 M 2-ME, and 0.45 M Tris, pH 6.8), and then boiled 10 min. Cellular debris was removed by centrifugation for 5 min at 14,000 rpm, and supernatants were transferred to fresh tubes. Extracts corresponding to 1.2–2 × 10^6 cell equivalents were loaded into each lane of an 8.5% SDS-PAGE gel and blotted after electrophoresis to Hybond-ECL nitrocellulose membrane (0.45 μm pore size; Amersham, Arlington Heights, IL) at 55 V for 5 h in transfer buffer (25 mM Tris, 192 mM glycine, and 15% methanol). Nonspecific binding was blocked by overnight incubation in BLOTTO (5% nonfat milk powder and 0.1% Tween 20 in PBS) at 4°C. Blots were probed with the anti-α-fodrin mAb 1622 at a dilution of 1/2,500 in BLOTTO for 1 h at room temperature. Filters were washed three times for 5 min each time with PBS/0.1% Tween 20 (PBS-T), then incubated for 30 min at room temp with BLOTTO containing a 1/2,500 dilution of HRP-conjugated sheep anti-mouse Ig (Amersham). Filters were washed extensively (once for 15 min, then twice for 5 min each time) with PBS-T, and the specific protein complexes were identified using the ECL-Western blotting detection system (Amersham). For subsequent analysis of PARP cleavage, blots were stripped for 30 min at 50°C in strip buffer (0.1 M 2-ME, 2% SDS, and 62.5 mM Tris-HCl, pH 6.7), washed extensively with PBS-T, incubated in BLOTTO O/N at 4°C, then probed as described above with the anti-human PARP mAb 60.815 at a dilution of

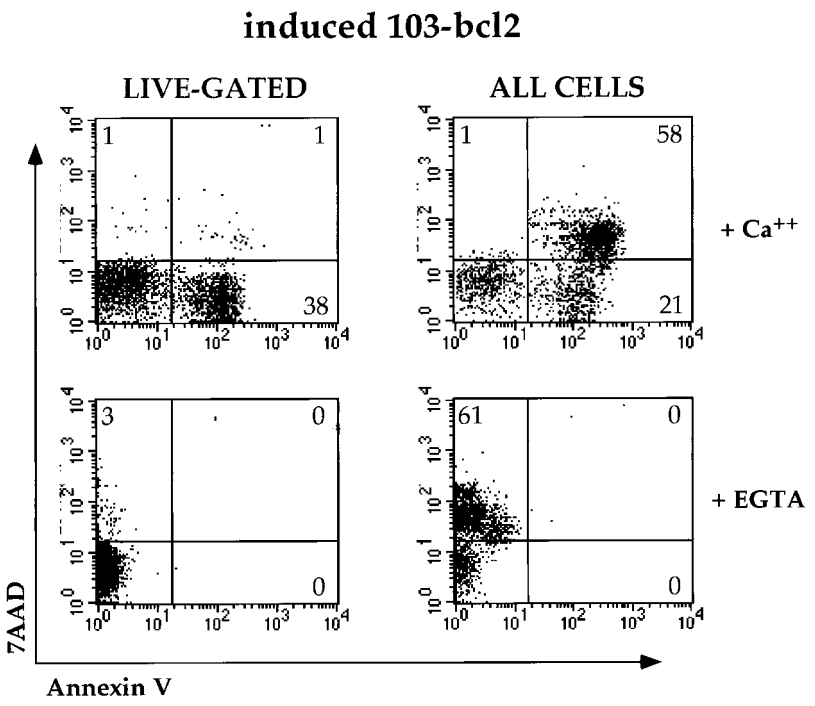

FIGURE 1. rAnV staining can be used to discriminate apoptotic, dead, and viable 103-bcl2 pro B cells. The temperature-sensitive pro-B cell line103-bcl2 was induced to undergo apoptosis by shifting the cells from 33°C to 39°C for 15 h. Cells were harvested, stained with FITC-AnV and 7AAD in the presence of $CaCl_2$ (*upper panels*) or EGTA (*lower panels*), and analyzed by flow cytometry. Data were gated on viable/early apoptotic cells based on their light scatter characteristics (*left panels*) or were analyzed ungated (*right panels*). The percentages of cells falling within each quadrant are indicated.

1/5,000. After washing, the blot was incubated with goat anti-human Ig-HRP at a 1/15,000 dilution, then developed by ECL. For anti-phosphotyrosine immunoblotting, cells were stimulated as noted in the text, washed twice in protein-free HBSS containing 1.5 mM $CaCl_2$ and 1 mM Na_3VO_4, lysed for 10 min on ice in TNT lysis buffer (1% Triton X-100, 150 mM NaCl, 50 mM Tris-Cl (pH 7.6), 1 mM Na_3VO_4, 1 mM PMSF, 1 μg/ml aprotinin, and 1 μg/ml leupeptin), then centrifuged to remove debris. Supernatants (from 10^6 cells/lane) were run on 11% acrylamide gels and transferred to nitrocellulose. Filters were blocked overnight in TBS/BSA (10 mM Tris-Cl (pH 8.0), 150 mM NaCl, and 2% BSA), then incubated at room temperature for 1 h with 1 μg/ml 4G10 diluted in TBS/BSA. The blot was washed three times (10 min each time) with PBS-T, incubated with sheep anti-mouse-Ig-HRP (1/6,000) for 30 min at room temperature, then washed three times with PBS-T (10 min each) and developed by ECL.

Immunofluorescence microscopy

Cells were stained (or not) with mAbs as indicated in the text, fixed for 30 min at room temperature in fresh 2% paraformaldehyde solution, then centrifuged and washed twice. For GM1 staining, fixed cells were incubated with FITC-CTx (8 μg/ml) for 30 min, then washed before analysis. Confocal microscopy was performed on a scanning confocal microscope system (model LSM 410, Carl Zeiss, Thornwood, NY).

Results

rAnV stains B cells induced to undergo apoptosis in vitro

We prepared rAnV and conjugated it to either FITC or biotin for use in flow cytometry (30). To confirm the ability of rAnV to detect cells undergoing apoptosis, we stained 103-bcl2, a temperature-sensitive Abelson virus-transformed pro-B cell line (32). This cell line can be induced to undergo apoptosis by shifting cells from the permissive temperature (33°C) to a nonpermissive temperature (39°C) (32). As predicted from previous studies (30), when FITC-rAnV is used in combination with the DNA-binding dye 7-aminoactinomycin D (7AAD; excluded from viable cells with an intact plasma membrane) to stain 103-bcl2 cells cultured at 39°C overnight, we can readily detect both apoptotic ($rAnV^+7AAD^-$) and dead ($rAnV^+7AAD^+$) cells (Fig. 1). The light scatter characteristics of the latter cells correlate well with their rAnV/7AAD profiles, as most of these are $FSC^{low}SSC^{int/high}$ (data not shown). Only sorted $rAnV^-7AAD^-$ (viable) cells and not $rAnV^+7AAD^-$ (apoptotic) cells incorporated [^{3}H]thymidine upon subsequent culture for 72 h at the permissive temperature (data not shown). The $rAnV^+7AAD^-$ cells also exhibited membrane blebbing and nuclear condensation, and their DNA displayed internucleosomal fragmentation, all characteristic features of apoptosis (30) (data not shown).

rAnV binds to viable B cells bearing a selectable BCR

Given that rAnV so clearly demarcates apoptotic 103-bcl2 cells in vitro, we proceeded to use this reagent to stain primary B cells directly ex vivo. We isolated BM cells and splenocytes from a variety of mice, including normal nontransgenic (non-Tg) mice and mice expressing transgenes encoding both the H and L chains of an Ab specific for the MHC class I molecule H-2K (clone 3-83) (26). The 3-83 Ab, isolated from a B-2 clone, binds to $H\text{-}2K^k$ with high affinity and to $H\text{-}2K^b$ with moderate affinity, but does not bind with appreciable affinity to $H\text{-}2K^d$ (34, 35). Thus, in $H\text{-}2^d$ 3-83 Tg mice or in $H\text{-}2^b$ $\beta_2m^{-/-}$ 3-83 Tg mice (whose cells lack surface expression of MHC class I molecules) (27), nearly all the immature BM B cells and mature peripheral B cells express the Tg BCR and stain with the 3-83 Id-specific mAb 54.1 (35, 36) (data not shown). However, in $H\text{-}2^b$ or $H\text{-}2^k$ 3-83 Tg mice, B cell development is arrested at an immature stage, and those Tg B cells remaining are $IgM^{low}IgD^-$ (14).

We used anti-B220-PE and FITC-rAnV to stain BM and splenic cells isolated from 3-83 Tg mice on both a negatively selecting background ($H\text{-}2^b$ $\beta_2m^{+/-}$) and a background permissive for the survival of cells expressing the Tg BCR ($H\text{-}2^b$ $\beta_2m^{-/-}$). Contrary to expectation, we found that most of the live-gated $B220^+$ cells in the $\beta_2m^{-/-}$ Tg BM and spleen bind rAnV despite the absence of a self Ag that might trigger apoptosis (Fig. 2). These Tg B cells bind rAnV at intermediate levels ($rAnV^{int}$): significantly higher than background staining in the absence of Ca^{2+}, but lower than the levels found on dead or dying cells (Fig. 2 and see below). Furthermore, a substantial proportion (~40–50%) of B cells in both non-Tg and $H\text{-}2^b$ $\beta_2m^{+/-}$ Tg BM and spleen also bind rAnV at intermediate levels (Fig. 2).

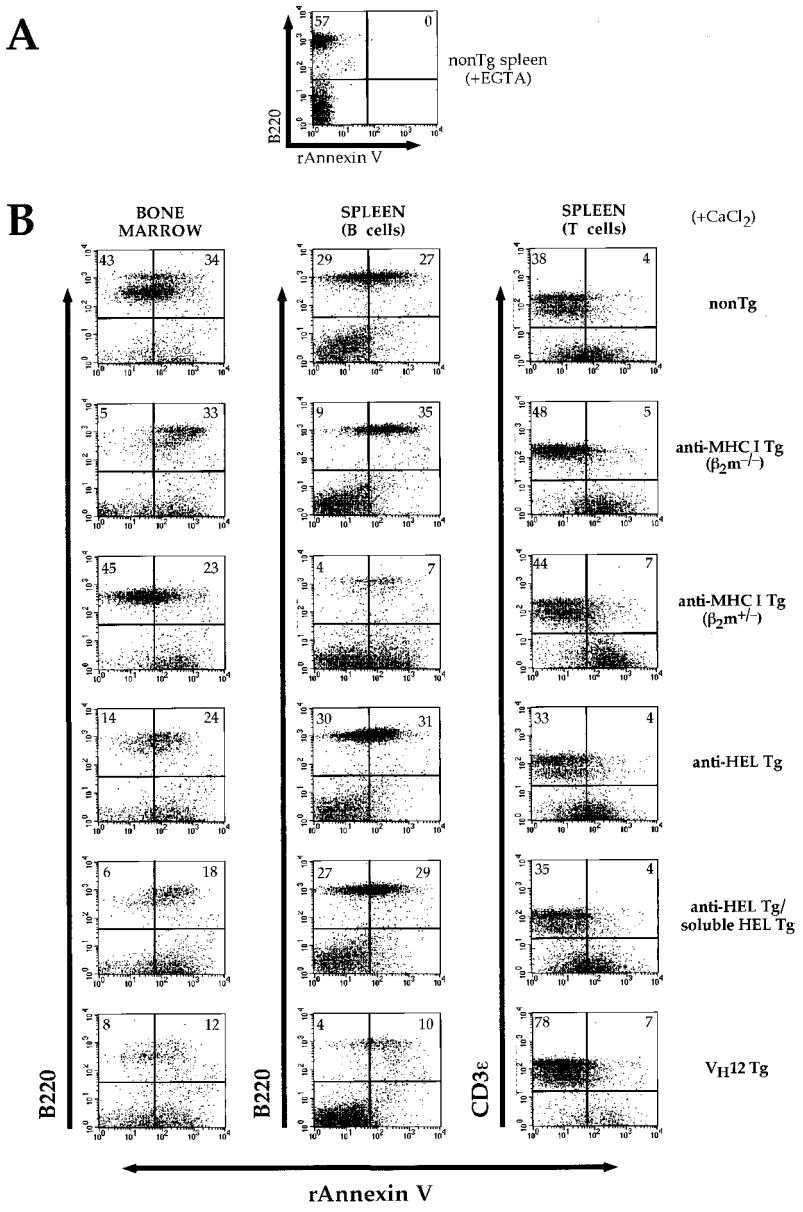

FIGURE 2. A large proportion of viable BM and splenic B cells bearing selectable H+L Ig Tg BCRs stain with FITC-rAnV. *A*, To establish background levels of rAnV staining in the absence of Ca^{2+}, splenocytes from a non-Tg mouse were stained with FITC-rAnV, anti-B220-PE, and anti-CD3ε-biotin followed by QR-SA in buffer containing EGTA and analyzed by flow cytometry. Similar profiles were obtained using cells from all the mice analyzed below. *B*, BM cells (*left column*) and splenocytes (*middle* and *right columns*) collected from a non-Tg (*top row*), H-2^b $\beta_2m^{-/-}$ 3-83 Tg (*second row*), H-2^b $\beta_2m^{+/-}$ 3-83 Tg (*third row*), anti-HEL Ig Tg (*fourth row*), anti-HEL/soluble HEL double-Tg (*fifth row*), or V_H12 Tg (*sixth row*) mice were stained and analyzed as described in *A*, except for the substitution of $CaCl_2$ in the buffer in place of EGTA. Note that the $\beta_2m^{-/-}$ genetic background (*second row*) is permissive to the 3-83 BCR, while the presence of H-$2K^b$ in the $\beta_2m^{+/-}$ mice (*third row*) leads to negative selection of the 3-83 Tg B cells. Data were gated on viable lymphocytes based on their light scatter characteristics; separate analyses confirmed that 95–99% of the $B220^+rAnV^+$ cells in this gate exclude 7AAD (data not shown). B220 vs rAnV profiles are shown for BM and spleen (*left* and *middle columns*), and CD3 vs rAnV profiles are shown for spleen (*right column*), with the percentage of cells in each of the upper quadrants indicated. The rAnV staining of B cells is highly reproducible; the data shown are representative of three (anti-HEL Tg) to 20 (3-83 and V_H12Tg) experiments, and we observed only minor mouse-to-mouse variation within each Tg strain.

To determine whether affinity for rAnV is an idiosyncrasy of B cells in the 3-83 Tg mice (and those in their non-Tg littermates), we also analyzed BM from Ig Tg mice expressing H and L chains with specificity for hen egg lysozyme (HEL) (28). Corroborating our results with 3-83 Tg mice, we found that in anti-HEL Ig Tg mice lacking the HEL Ag, a large proportion of BM B cells binds FITC-rAnV (Fig. 2). We also stained cells from anti-HEL/soluble HEL (sHEL) double-Tg mice, where the presence of HEL as a self Ag induces anergy in the B cells expressing the anti-HEL BCR (28). Again, a large fraction of the anergic Tg B cells in these mice bound FITC-rAnV (Fig. 2).

Finally, we examined V_H12 Tg mice, which bear an IgH transgene isolated from a B-1 cell clone specific for PC. In V_H12 Tg mice, the rearranged IgH transgene efficiently mediates positive selection of developing B cells into the B-1 cell subset (29). When we stained BM and spleen cells from these mice with anti-B220-PE and FITC-rAnV, we again found that a large fraction of Tg BM cells bound rAnV, as did nearly all the splenic B-1 cells (Fig. 2 and our manuscript in preparation). Interestingly, we did not observe similar rAnV binding on splenic T cells. In general, $<10\%$ of $CD3^+$ splenic T cells (Fig. 2) or thymocytes (data not shown) in any of the mice we analyzed (including TCR Tg mice; our manuscript in preparation), bind rAnV above background levels. Thus, PS exposure on nonapoptotic cells is not a general characteristic of all lymphocytes, but is instead a feature that is relatively specific to the B cell lineage.

We performed two experiments to address the binding specificity of rAnV. First, FITC-rAnV was preincubated with liposomes prepared from a panel of phospholipids (33) before staining BM cells. The rAnV binding to viable ($7AAD^-$) non-Tg or H-2^d 3-83 Tg BM B cells was strongly inhibited by 5 μM PS-containing liposomes and partially inhibited by PI (another negatively charged phospholipid), but was virtually unaffected by PC, PtE, phosphatidic acid, or SM (Fig. 3*A*). Thus, rAnV is binding in a specific fashion to negatively charged phospholipids, especially PS, exposed on the surface of BM B cells. Second, we sought to determine whether rAnV was binding to a B cell-specific lipoprotein rather than to the lipid membrane itself. Splenocytes were incubated with pronase before staining with anti-CD19-PE and rAnV-FITC. As shown in Fig. 3*B*, pronase treatment completely

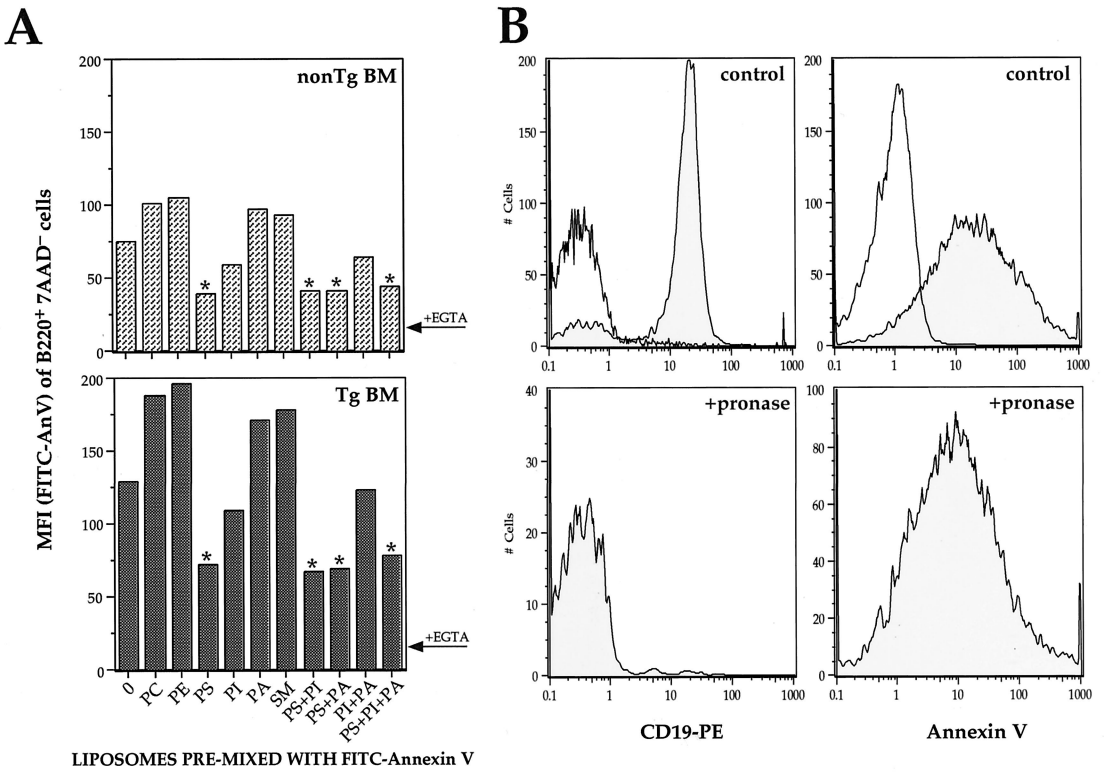

FIGURE 3. The specificity of rAnV staining. *A*, Preincubation of FITC-AnV with PS-containing liposomes inhibits its binding to BM B cells. Non-Tg (hatched bars, *top panel*) or H-2^d 3-83 Ig Tg (shaded bars, *lower panel*) BM cells were stained with anti-B220-PE, 7AAD, and FITC-rAnV premixed with the liposomes indicated (as described in *Materials and Methods*). Data were gated on $B220^+7AAD^-$ cells. The mean fluorescence intensity (MFI) in the FITC channel of the gated populations is plotted against the type of liposome(s) mixed with the FITC-AnV before staining. Samples tested with PS-containing liposomes are indicated by asterisks. The MFI in the FITC channel for cells stained in the presence of EGTA was generally about 10, as indicated by the arrows. Comparable patterns of liposome-mediated inhibition of AnV staining were observed on splenocytes from the same mice. Similar results were obtained in three independent experiments. *B*, Pronase treatment fails to significantly diminish FITC-AnV binding to splenic B cells. Purified splenocytes from a non-Tg mouse were incubated for 5 min at 37°C without (control) or with (+ pronase) pronase, washed extensively, and stained with anti-CD19-PE (*left panels*) and FITC-rAnV (*right panels*). Control anti-CD19-PE staining (shaded) is compared with unstained cells (unshaded), and control rAnV staining performed in the presence of Ca^{2+} (shaded) is compared with staining performed in the presence of EGTA (unshaded). The data were gated on live cells based on forward and side scatter.

eliminated anti-CD19 staining, but only reduced rAnV staining 2-fold. Thus, rAnV is almost certainly binding to PS in the plasma membrane itself.

Most rAnV-binding B cells are not apoptotic

Our initial experiments suggested that most of the B cells that bind rAnV in Ig Tg and non-Tg BM are not undergoing apoptosis. To confirm this observation, we examined rAnV-binding BM B cells using a wide variety of independent assays to detect apoptosis. One of the hallmarks of the later stages of apoptosis is internucleosomal DNA cleavage (37). This form of DNA degradation can be detected either by agarose gel electrophoresis or by the TUNEL assay (38). Cellular DNA isolated from FACS-sorted $rAnV^{int}B220^+7AAD^-$ H-2^d 3-83 Tg BM cells did not exhibit laddering on agarose gels (data not shown). Likewise, when we subjected non-Tg or H-2^d 3-83 Tg BM cells to TUNEL analysis, we found that only a small proportion of rAnV-binding cells were also $TUNEL^+$, and that these cells stained brightly with rAnV ($rAnV^{high}$; Fig. 4*A*). Virtually none of the dominant $rAnV^{int}$ B cell population is $TUNEL^+$. Similar results were obtained using splenocytes from V_H12 Tg mice, again ruling out potential idiosyncrasies with the 3-83 Tg mice (data not shown). These results are in striking contrast to the staining patterns observed for induced 103-bcl2 cells, in which nearly all the rAnV-binding cells are also $TUNEL^+$ (Fig. 4*A*). We also examined sorted $rAnV^+7AAD^-$ 3-83 Tg BM B cells by fluorescence microscopy after staining the cells with the DNA-binding dye 4′,6-diamidino-2-phenylindole to mark nuclei. These cells displayed a normal nuclear staining pattern, and their general morphology did not reveal the membrane blebbing that generally accompanies apoptosis (data not shown).

We proceeded to assay the $rAnV^+$ BM B cells for earlier apoptotic events. Apoptotic cells lose their mitochondrial transmembrane potential ($\Delta\psi_m$), an event that generally occurs concomitant with or just before surface exposure of PS (39). To detect a possible loss of $\Delta\psi_m$ in $rAnV^+$ B cells, we stained non-Tg and 3-83 Ig Tg BM cells with the lipophilic dye $DiOC_6$ (40). Cells that have lost their $\Delta\psi_m$ are unable to retain $DiOC_6$, as we observed in control experiments with induced 103-bcl2 cells (Fig. 4*B*). In distinction to apoptotic 103-bcl2 cells, the majority of both non-Tg and 3-83 Tg $rAnV^{int}$ BM B cells retain $DiOC_6$ at high levels (Fig. 4*B*).

Merocyanine 540 (MC540) is a dye that intercalates into loosely packed lipid membranes (41). Cells at the later stages of apoptosis begin to lose the integrity of their lipid arrangement and will bind MC540 (42). As shown in Fig. 4*C*, apoptotic 103-bcl2 cells that bind the highest levels of rAnV also stain with MC540. Similarly, in 3-83 Tg or non-Tg BM, the cells binding the highest amounts of rAnV also bind MC540. The dominant population of $rAnV^{int}$ Tg B cells falls into both $MC540^+$ and $MC540^-$ subsets (Fig. 4*C*). These results indicate that although the majority of these B cells maintain their overall membrane integrity, there are alterations in

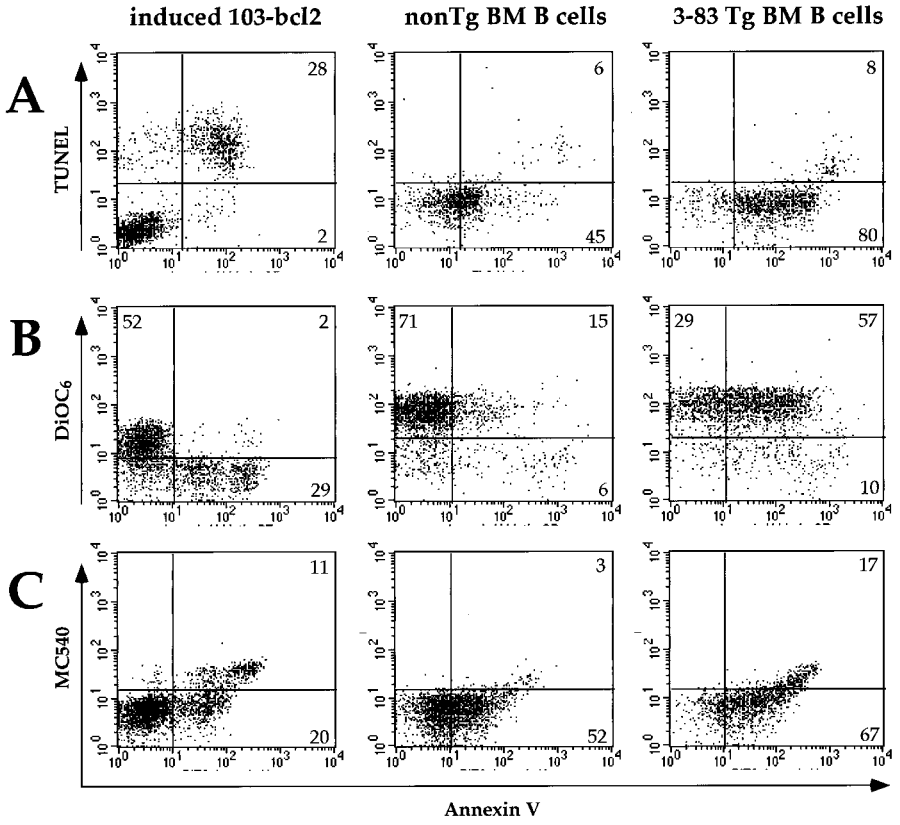

FIGURE 4. Most rAnV-binding primary B cells do not display other characteristic markers of apoptosis. *A*, 103-bcl2 cells shifted to 39°C for 12 h (*left panel*) and BM cells from an H-2^d 3-83 Ig Tg (*right panel*) or a non-Tg littermate (*middle panel*) were stained with anti-B220-PE (BM cells only) and rAnV-biotin followed by QR-SA, then were fixed, permeabilized, and tested for the characteristic DNA breaks of apoptosis using the TUNEL assay. The TUNEL vs rAnV FACS profiles for live-gated 103-bcl2 cells or for live-gated B220$^+$ BM cells are shown. Note that the difference in the size and granularity of 103-bcl2 cells vs BM B cells requires separate cytometer settings and precludes a direct comparison of their respective rAnV staining levels. *B*, Cells described in *A* were stained with $DiOC_6$, anti-B220-PE (BM cells only) and rAnV-biotin followed by PE-SA (103-bcl2) or QR-SA and analyzed on a FACScan. The $DiOC_6$ vs rAnV FACS profiles are shown for cells gated as described in *A*. *C*, Cells described in *A* were stained with FITC-rAnV, MC540, and (BM cells only) CD19-biotin followed by QR-SA. The MC540 vs rAnV FACS profiles for live-gated 103-bcl2 cells or live-gated CD19$^+$ BM cells are shown. The percentage of rAnV-binding cells varies in *A*, *B*, and *C*, because these sets of data were obtained in separate experiments using different groups of mice.

the lipid packing on those cells binding the highest levels of rAnV (see *Discussion*).

Because most cytometric assays for apoptosis measure events that occur after the exposure of PS, we next turned to biochemical analyses of rAnV-binding B cells. One of the very earliest events in cells undergoing apoptosis is the cleavage of various protein substrates by caspases (reviewed in Ref. 43). The DNA repair enzyme PARP is cleaved almost immediately after the onset of apoptosis (44). A second target protein is α-fodrin (nonerythroid spectrin), a ubiquitous membrane-associated cytoskeletal protein whose cleavage during apoptosis is thought to play a role in membrane blebbing (45). To determine whether these proteins have been cleaved in rAnV-binding BM B cells, we prepared whole cell lysates from immunoaffinity-purified CD19$^+$rAnV$^+$ H-2^d 3-83 Tg BM B cells, non-Tg CD19$^+$ BM cells, or induced 103-bcl2 cells and subjected them to immunoblot analysis with Abs specific for α-fodrin or PARP. Although extensive cleavage of α-fodrin (240 kDa) into its 150- and 120-kDa products is clearly evident in the induced 103-bcl2 sample, none of the 150-kDa product and only a small amount of the 120-kDa product were found in the BM B cell samples (Fig. 5*A*). The presence of the 150-kDa product is most indicative of active apoptosis, because it is only transiently formed (46). The 120-kDa band is more ubiquitous, as it is generated even in the largely rAnV$^-$ splenocyte population (Fig. 5*A*) and in purified splenic T cells that are essentially rAnV$^-$ (data not shown). Strikingly, no degradation of PARP is detectable among rAnV$^+$ BM B cells, in clear contrast to the induced 103-bcl2 cells, which exhibit extensive PARP cleavage (Fig. 5*B*). Thus, by multiple independent criteria, these rAnV-binding B cells are not apoptotic.

PS externalized on viable B cells co-caps with the BCR

To examine the distribution of PS on the surface of B cells, we used fluorescence microscopy to analyze both Ig Tg and non-Tg splenocytes costained with FITC-rAnV and goat anti-mouse-IgM-PE. Cells kept on ice and examined while still cold exhibited a homogeneous staining pattern for both PS and IgM (Fig. 6*A*). However, as the cells warmed to room temperature and the IgM molecules began to cap at one pole of the cell (46), the PS clearly traveled with the IgM into the cap (Fig. 6*B*). This co-capping phenomenon did not depend upon cross-linking PS with rAnV, because we also found PS in caps of IgM formed before we stained with rAnV (Fig. 6*C*). The co-capping we observed is specific; if we first cross-linked IgM on splenic B cells, then fixed the cells and stained with FITC-rAnV and an Ab to MHC class I, the PS entered the IgM cap while the MHC molecules remained homogeneously distributed (Fig. 6*D*). We also found that B220

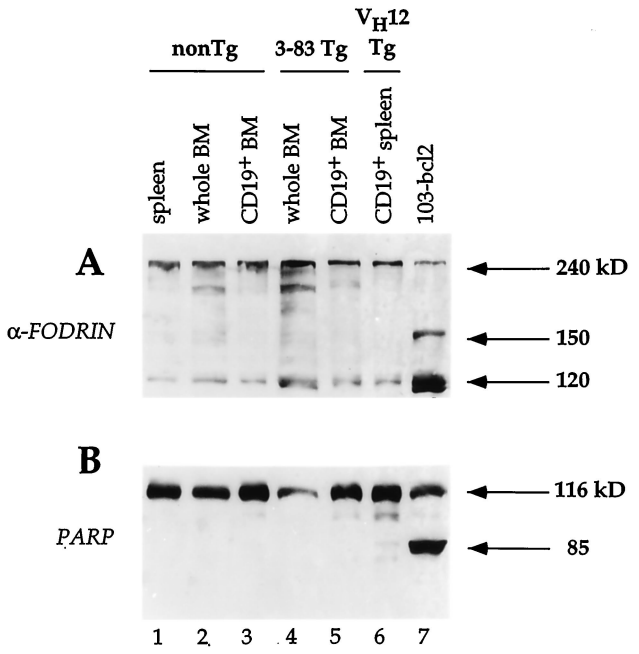

FIGURE 5. The rAnV-binding B cells do not exhibit protease activities indicative of early apoptosis. *A*, Western blot analysis of α-fodrin cleavage in whole cell lysates from unfractionated BALB/c splenocytes (*lane 1*), whole BM (*lane 2*), and $CD19^+$ BM (85% $B220^+$/40% $rAnV^+$; *lane 3*); from H-2^d 3-83 Ig Tg whole BM (*lane 4*) and $CD19^+$ BM (70% $B220^+$/65% $rAnV^+$; *lane 5*); from V_H12 Tg $CD19^+$ spleen (90% $B220^+rAnV^+$; *lane 6*); and from induced 103-bcl2 cells (65% $rAnV^+$; *lane 7*). The locations of intact α-fodrin (240 kDa) and its dominant cleavage products (150 and 120 kDa) are indicated. $CD19^+$ cells were isolated using magnetic immunoaffinity columns; similar results were obtained using FACS-sorted $B220^+rAnV^+7AAD^-$ 3-83 Ig Tg BM (data not shown). *B*, The blot in *A* was stripped, washed, and incubated with anti-PARP antisera, as described in *Materials and Methods*. The locations of PARP (116 kDa) and its major cleavage product (85 kDa) are indicated.

(CD45R) was generally absent from PS/IgM caps in anti-IgM-treated cells (data not shown; see *Discussion*). Thus, to our surprise, a lipid probe (rAnV) and a protein probe (anti-IgM Ab) simultaneously altered their membrane distribution in capped B cells.

The observation that PS redistributes along with the BCR in capped B cells led us to consider whether both the BCR and PS were colocalized within "lipid rafts." These dynamic membrane microdomains (<70 nm) were originally discovered on nonlymphoid cells and are known by several additional terms, including glycolipid-enriched membrane domains and detergent-insoluble glycolipid-enriched membrane domains (47–49). Rafts are characterized by high concentrations of glycosphingolipids (e.g., GM1), cholesterol, GPI-anchored proteins, and several molecules involved in signal transduction. It has been proposed that these rafts move within the lipid bilayer and function as platforms for the attachment of proteins whose localization and clustering may be critical for signal transduction.

One of the components of lipid rafts is the GM1 glycosphingolipid, which binds the β subunit of CTx (50). FITC-labeled CTx can therefore be used to stain fixed cells and directly visualize these raft domains (51, 52). To test whether GM1 is present in IgM/PS caps, we stimulated splenocytes with unlabeled anti-IgM, stained them with rAnV-biotin followed by Texas Red-streptavidin (TR-SA), then fixed the cells and stained them with FITC-CTx. As shown in Fig. 6*E*, PS and GM1 colocalize in the anti-IgM-induced caps. Interestingly, we found that PS, IgM, and GM1 also colocalize on anti-IgM-treated anergic B cells from an anti-HEL/sHEL double-Tg mouse (Fig. 6*F*) (28). This indicates that anergic B cells are still capable of assembling IgM into rAnV- and CTx-binding domains, and implies that their functional deficiencies lie downstream of this early event (53, 54).

PS, IgM, and GM1 are frequently co-capped in vivo on B-1 cells and anergic B-2 cells

When we assessed the phenotypes of splenocytes directly ex vivo by fixing the cells immediately after isolation and staining them with FITC-CTx and anti-IgM-PE, we frequently found cells in the anti-HEL Ig/sHEL double-Tg mice that had already capped their surface IgM in vivo, presumably mediated by their interaction(s) with Tg sHEL protein (Fig. 6*H*). This in vivo capping was never observed in the anti-HEL Ig Tg B cells, which developed in the absence of the sHEL Ag (Fig. 6*G*). Pre-capping in vivo was also evident in many of the splenic B-1 cells from the V_H12 Ig Tg mice (data not shown), whose BCR recognizes PC, a ubiquitous lipid species (Fig. 2). This constitutive capping of the BCR in B-1 cells and in anergic B-2 cells may have implications for the signaling activities of the BCR under these physiologic circumstances (see *Discussion*).

Disruption of PS/IgM co-capping interferes with BCR signaling events

Having found that PS associates with IgM undergoing capping in anti-Ig-treated B cells, we investigated whether this association has any influence on signaling by the BCR. We stained splenic B cells with rAnV-biotin and then treated the washed cells with SA for 20 min at 37°C. Confocal microscopy revealed that this treatment resulted in clustering of PS on the B cell surface without significantly affecting the distribution of surface IgM (Fig. 7*A*). We then incubated rAnV- plus SA-treated or untreated splenocytes with various amounts of a cross-linking anti-IgM Ab for 5 min at 37°C. Lysates from these cells were prepared and analyzed for changes in the pattern of tyrosine-phosphorylated proteins by Western blot (Fig. 7*B*). As expected, B cells treated with as little as 0.6 μg/ml anti-IgM showed a striking increase in the levels of many phosphorylated species compared with the pattern seen in lysates from control unstimulated cells (Fig. 7*B*, *lanes 5, 7, 9,* and *11*). Notably, one phosphoprotein with an approximate molecular mass of 16 kDa present in lysates of unstimulated cells lost its phosphotyrosine(s) after anti-IgM treatment (Fig. 7*B*, compare *lanes 1* and *5*). Pretreatment of the B cells with rAnV-biotin and SA resulted in at least one striking change in this pattern; phosphorylation of the 16-kDa protein was maintained regardless of surface IgM cross-linking, implying that the preclustering of PS disrupts the dephosphorylation of this protein after BCR stimulation. If we co-cross-link PS and IgM by adding SA to cells prestained with rAnV-biotin and anti-IgM-biotin, the 16-kDa species is almost completely dephosphorylated (Fig. 7*B*, *lane 14*), as it is with anti-IgM-biotin and SA alone (*lane 13*). Pretreatment of B cells with rAnV-biotin and SA resulted in several additional changes in the phosphorylation pattern, including the accelerated disappearance (i.e., from 10 to 4 μg/ml anti-IgM) of a phosphoprotein of ~150 kDa (Fig. 7*B*, compare *lanes 7* and *8*). This result indicates that sequestration of PS by rAnV cross-linking also interferes with kinase activity in anti-IgM-treated B cells. Thus, we conclude that the presence of PS or of membrane alterations associated with rAnV binding can influence the nature of the BCR signal.

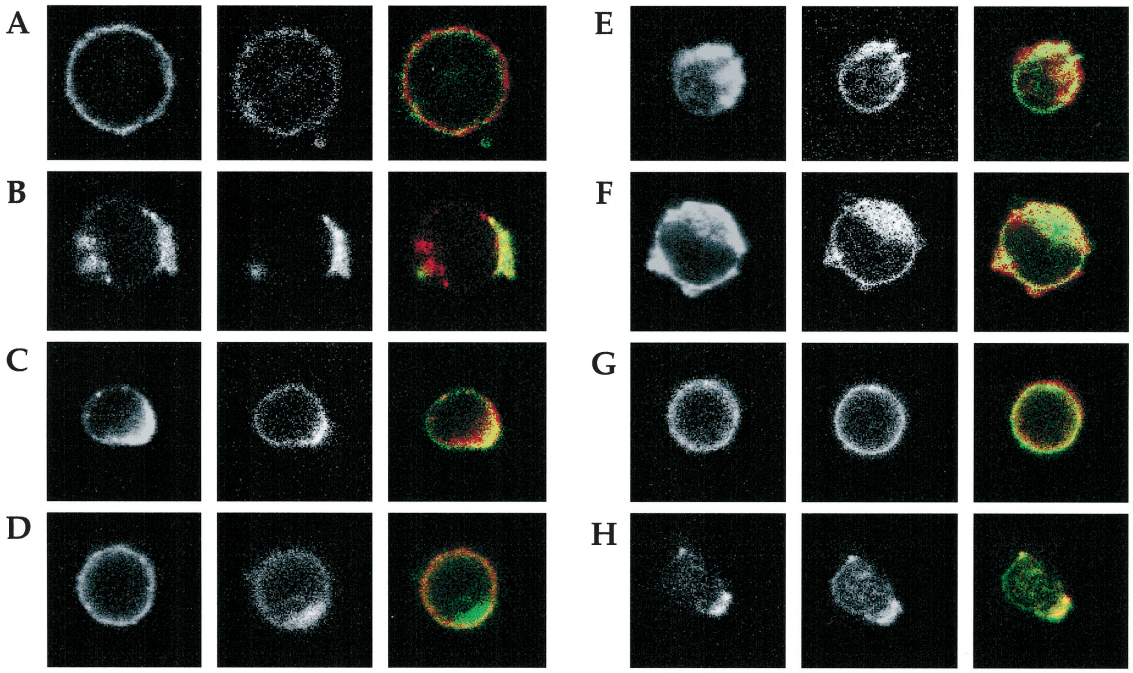

FIGURE 6. PS exposed on viable B cells co-caps with IgM after IgM cross-linking and colocalizes with GM1, a component of lipid rafts. Confocal microscopy analysis of splenocytes from anti-HEL Ig Tg (*A*, *C*, *D*, and *G*), V_H12 Ig Tg (*B*), non-Tg (*E*), or anti-HEL/sHEL double Tg (*F* and *H*) mice stained as follows. *A*, Cells were fixed immediately after isolation and stained with FITC-rAnV and goat anti-mouse IgM-PE. *B*, Cells stained with FITC-rAnV and goat anti-mouse IgM-PE were incubated at 37°C for 30 min, then fixed. *C*, Cells were incubated with goat anti-mouse IgM-PE for 5 min at 37°C, then fixed and stained with FITC-rAnV. *D*, Cells were incubated with unlabeled goat anti-mouse IgM for 10 min at 37°C, then fixed and stained with FITC-rAnV and anti-MHC class I (K^b) followed by goat anti-mouse IgG2a-PE. *E* and *F*, Cells were prestained with rAnV-biotin, washed, incubated with unlabeled goat anti-mouse IgM and TR-SA for 15 min, then fixed and stained with FITC-CTx. *G* and *H*, Cells were fixed and stained with goat anti-mouse IgM-PE and FITC-CTx. The *first panel* in each set of three depicts red (PE and TR) fluorescence; the *middle panels* show green (FITC) fluorescence, and the *third panel* depicts the merger of the red and green images; colocalization is indicated by yellow fluorescence in the merged images. Except for specific differences noted in the text (*G* and *H*), similar results for each staining protocol were obtained using splenocytes from all mice tested; representative images are shown.

Discussion

PS exposure can be uncoupled from apoptosis in the B cell lineage

The exposure of PS on the surface of apoptotic cells is a well-documented phenomenon (reviewed in Ref. 21). We report here our surprising finding that viable developing and mature B cells bearing a BCR that can mediate positive selection, and thus inclusion of a B cell into the peripheral repertoire, display an altered membrane structure that allows rAnV binding to the plasma membrane. Furthermore, we have shown that $rAnV^{int}$ B cells do not display any of the other well-known biochemical or morphologic characteristics associated with apoptosis, including internucleosomal DNA fragmentation, loss of mitochondrial $\Delta\psi_m$, nuclear chromatin condensation, or the cleavage of proteins such as α-fodrin and PARP (Figs. 4 and 5 and data not shown). Therefore, the exposure of PS can be unlinked from the apoptosis pathway in lymphocytes. Our data do not imply, however, that rAnV cannot be used to detect apoptotic B cells. In addition to its clear utility in identifying apoptotic B cells in vitro (25) (Fig. 1), this reagent does detect small populations of $rAnV^{high}$ $TUNEL^+$ $DiOC_6^-$ BM B cells that apparently are undergoing apoptosis (Fig. 4, *A* and *B*).

How do PS^+ B cells escape engulfment by BM macrophages?

It is believed that morphological changes on the surface of cells dying in vivo, including the exposure of PS, provide key signals to neighboring phagocytes that induce these scavengers to engulf and digest them (reviewed in Ref. 55). This specialized process of cellular housekeeping prevents the induction of inflammation and tissue damage that can arise when cells undergo a necrotic death. If $TUNEL^+$ self-reactive thymocytes can be found within thymic macrophages (17), how can B cells with exposed PS escape phagocytosis by BM macrophages? One possibility is that the PS receptors expressed by macrophages may be dependent upon the overall density of PS on the target cell, allowing $rAnV^{int}$ B cells to survive in an environment where $rAnV^{high}$ cells are targets for destruction. However, it seems more likely that $rAnV^{int}$ B cells lack additional surface changes present on apoptotic cells that are required to trigger phagocytosis (55). At least five macrophage surface molecules, including the vitronectin receptor $\alpha_v\beta_3$ integrin, CD36; the class A scavenger receptor, CD14; and the ATP binding cassette transporter, ABC-1, have been shown to be involved in the removal of apoptotic cells, in some cases through adhesive bridging interactions with extracellular matrix proteins on the apoptotic target (21, 55). In addition to PS redistribution on apoptotic cells, some carbohydrate changes at the cell surface may provide important ligands for phagocytes (56). It is therefore probable that the viable PS^+ BM B cells we have identified (Fig. 2) lack the full spectrum of requisite ligands for the surveying macrophages (21, 55, 57).

The role of PS associated with the BCR

Mature B cells triggered through their Ag receptors initiate a signaling cascade characterized by the phosphorylation and dephosphorylation of multiple cellular proteins. To achieve this signal amplification, IgM is associated with several accessory molecules, including Igα (CD79α) and Igβ (CD79β), which trigger Src and Syk family tyrosine kinases, the phosphatases CD45 (B220) and

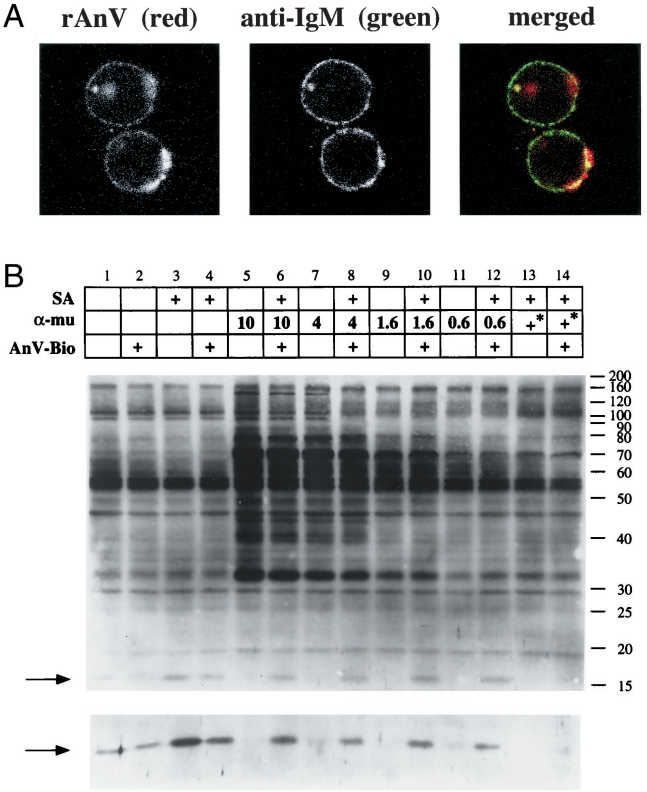

FIGURE 7. rAnV pretreatment alters the signaling properties of the BCR. *A*, Confocal microscopic analysis of B cells pretreated with rAnV-biotin and SA. Splenocytes from a V_H12 Tg mouse were stained on ice with rAnV-biotin, washed, and treated with PE-SA for 30 min at 37°C, returned to ice, stained with anti-IgM-FITC for 15 min, then fixed and analyzed by confocal microscopy. The PE (rAnV; *left panel*), FITC (IgM; *middle panel*), and coincident fluorescence (*right panel*) patterns are shown. Results are representative of analyses of cells from several types of mice (data not shown). *B*, Splenocytes from an anti-HEL Ig Tg mouse were prestained with rAnV-biotin (*lanes 2, 4, 6, 8, 10,* and *12*), washed, and incubated with (*lanes 4, 6, 8, 10,* and *12*) or without (*lane 2*) 20 μg/ml streptavidin for 20 min at 37°C. After the 20-min incubation, these rAnV-stained cells or unstained splenocytes (*lanes 5, 7, 9,* and *11*) were incubated with 10 μg/ml (*lanes 5* and *6*), 4 μg/ml (*lanes 7* and *8*), 1.6 μg/ml (*lanes 9* and *10*), or 0.64 μg/ml (*lanes 11* and *12*) goat anti-mouse IgM antisera for 5 min at 37°C. Negative controls included unstained cells incubated with SA alone (*lane 3*) or medium alone (*lane 1*) or cells stained with rAnV and incubated with SA (*lane 4*). Co-cross-linking of PS and IgM was achieved by staining cells with rAnV-biotin (*lane 14*) and/or goat anti-mouse IgM-biotin (*lanes 13* and *14*), washing, then incubating the cells for 10 min at 37°C with SA. Note that this treatment protocol (asterisks) might be expected to yield a less potent signal than that achieved using soluble anti-IgM (*lanes 5–12*). All cells were lysed immediately after incubation in buffer containing protease and phosphatase inhibitors. The lysates were analyzed by Western immunoblotting as described in *Materials and Methods*.

SH2-containing phosphatase-1 (SHP-1) (via its association with CD22), and the costimulatory molecules CD40, CD19, and CD21 (54, 58, 59). Our results suggest that PS exposed on the surface of viable B cells may play a role as a component of membrane microdomains (Fig. 6 and see below). Upon cross-linking with the appropriate Abs, externalized PS co-caps with several proteins expressed on B cells, including IgM, CD19, and MHC class I, although PS seems to co-cap most efficiently with IgM (data not shown and Fig. 6). Importantly, disruption of the activation-induced cosegregation of PS and IgM (by pretreating B cells with rAnV-biotin and SA) led to at least two notable changes in the phosphotyrosine patterns in lysates from cells subsequently stimulated with anti-IgM (Fig. 7). Thus, we postulate that PS is an important component of the membrane remodeling machinery in B lymphocytes required to achieve optimal association of signaling molecules with their intracellular targets.

Our results parallel several recent studies aimed at understanding the three-dimensional structure of the synapse between T cells and APC (52, 60–64). Discrete membrane microdomains, often referred to as lipid rafts, have been associated with signal transducing molecules in both nonlymphoid and lymphoid cells. Using FITC-CTx to detect GM1 in sphingolipid-cholesterol-rich rafts, one group demonstrated that these rafts aggregate in the zone of contact between T cells and anti-CD3-coated beads (52). Furthermore, these studies showed that CD28 exerts its costimulatory effects on T cells by recruiting rafts into the TCR/APC contact site, rather than by integrating CD28 and TCR signals in the nucleus, to affect gene expression (52, 62). The membrane compartmentalization between rafts and nonrafts is required for efficient T cell activation, probably by recruiting intracellular kinases to the synapse while maintaining segregation of phosphorylated substrates from phosphatases (60, 64). Interestingly, in line with a report that the phosphatase CD45 is excluded from lipid rafts in T cells (65), we found that B220 (CD45R) is generally absent from PS/IgM caps in anti-IgM-treated cells (data not shown).

It remains unclear whether the association of IgM and PS in the B cell membrane precedes signaling through the BCR or whether this association is induced by BCR signaling. Experiments to address this question, using fluorescence resonance energy transfer, are currently in progress. It will also be of interest to elucidate further the mechanism by which PS externalization is controlled in healthy cells, perhaps by regulated expression of the aminophospholipid translocase or scramblase enzymes known to affect lipid movement in the plasma membrane (66).

Although very few resting mature T cells or thymocytes bind rAnV ex vivo (Fig. 2 and data not shown), T cells activated with Con A in vitro show a uniform increase in rAnV-FITC binding (data not shown). Interestingly, the PS molecules exposed on Con A blasts or on the small subset of splenic T cells that bind rAnV (Fig. 2) also migrate into anti-CD3- or anti-Thy-1-induced caps (data not shown). The infrequency of resting T cells compared with resting B cells that bind rAnV in vivo (Fig. 2) might reflect developmentally regulated differences in the signaling pathways within B and T cells.

Endocytosis of IgM molecules bound to their cognate Ag leads to Ag processing and presentation to T cells and is therefore an integral part of the immune response. In addition to their role in concentrating appropriate signaling molecules, rafts in membranes are thought to function in sorting and trafficking transmembrane proteins through the endocytic pathway (67). Our confocal experiments have revealed that PS tagged with FITC-rAnV is not only capped, but is also internalized with the BCR on anti-IgM-treated B cells (data not shown). This suggests that PS may play a unique and significant functional role in B cell Ag presentation and might further explain its presence on a greater fraction of B cells vs. T cells.

What is the nature of the altered membrane structure on rAnV-binding B cells?

Although the liposome binding inhibition experiments (33) indicated that FITC-rAnV binding to B cells is strongly inhibited by preincubation of this reagent with PS-containing liposomes (Fig. 3*A*), it remains possible that rAnV binding reflects something other than PS externalization on these cells. It is unlikely that rAnV is binding to a lipid-modified glycoprotein, because binding was not

affected by pretreatment of cells with pronase (Fig. 3*B*). rAnV may bind an additional, as yet unidentified, lipid bearing a binding site identical or overlapping with that on PS. Alternatively, rAnV may be detecting a specialized arrangement of lipids in the membrane, perhaps a shift from a typical lamellar bilayer to hexagonal phases, for instance (reviewed in Ref. 68). This hypothesis is supported by our observation that a significant fraction (generally 20–25%) of rAnV-binding B cells also stain with MC540 (Fig. 4*C*), a dye that is sensitive to the molecular packing of membrane lipids and that intercalates into loosely packed lipid membranes (69). An altered lipid arrangement in localized regions of contact with Ag or with other cells may increase the efficiency of delivering appropriate signals to the B cell (Fig. 7*B*), as has been shown for T cells (52, 62). As discussed above, it seems reasonable to postulate that the changes in membrane structure revealed by rAnV and CTx on anti-IgM-stimulated cells (Fig. 6) may be analogous to those observed in T cells receiving costimulatory signals (52, 62).

Caps containing IgM, PS, and GM1 exist on B-1 cells and anergic B-2 cells ex vivo

Both B-1 and anergic B-2 cells are thought to receive continuous stimulation through their Ag receptors. In the B-1 lineage, this stimulus is thought to come from a low affinity interaction of the BCR with self Ag, which may play a role in the initial selection of these cells into the B-1 lineage (29). The BCR signaling differs between B-1 and B-2 cells, especially with respect to synergy between IgM and CD19 (70). Anergic B-2 cells also display signaling defects specific to the BCR as opposed to other accessory molecules, such as CD40 and cytokine receptors (71, 72). Our surprising finding that IgM, PS, and GM1 are cocapped in B-1 and anergic B-2 cells examined immediately ex vivo (Fig. 6) may offer an insight as to the mechanism of these signaling differences. The BCR may be sequestered from interaction with other regulatory surface receptors due to its highly focal distribution in the membrane, leading to alterations in B cell signaling behavior. Further experimentation will be required to determine which other signaling molecules are specifically excluded from or included within these BCR domains.

Acknowledgments

We thank Drs. T. Behrens, S. Clarke, C. Goodnow, D. Nemazee, D. Scott, and M. Soloski for providing or making available the various strains of mice used in these studies; T. Grdina, N. Rosenberg, and M. Soloski for gifts of cell lines and reagents; L.-Y. Hsu, H.-E. Liang, J. Lauring, and F. Polleux for helpful discussions; and P. Fink, C. Blish, N. Shastri, and members of the Schlissel laboratory for insightful comments on the manuscript.

References

1. Rajewsky, K. 1996. Clonal selection and learning in the antibody system. *Nature 381:751.*
2. Schatz, D. G., M. A. Oettinger, and M. S. Schlissel. 1992. V(D)J recombination: molecular biology and regulation. *Annu. Rev. Immunol. 10:359.*
3. Fang, W., D. L. Mueller, C. A. Pennell, J. J. Rivard, Y. Li, R. R. Hardy, M. S. Schlissel, and T. W. Behrens. 1996. Frequent aberrant immunoglobulin gene rearrangements in pro-B cells revealed by a *bcl-xL* transgene. *Immunity 4:291.*
4. Hardy, R. R., C. E. Carmack, Y. S. Li, and K. Hayakawa. 1994. Distinctive developmental origins and specificities of murine CD5$^+$ B cells. *Immunol. Rev. 137:91.*
5. Tarlinton, D. 1994. B-cell differentiation in the bone marrow and the periphery. *Immunol. Rev. 137:203.*
6. Hardy, R. R., K. Hayakawa, M. Shimizu, K. Yamasaki, and T. Kishimoto. 1987. Rheumatoid factor secretion from human Leu-1$^+$ B cells. *Science 236:81.*
7. Mercolino, T. J., L. W. Arnold, L. A. Hawkins, and G. Haughton. 1988. Normal mouse peritoneum contains a large number of Ly-1$^+$ (CD5) B cells that recognize phosphatidyl choline: relationship to cells that secrete hemolytic antibody specific for autologous erythrocytes. *J. Exp. Med. 168:687.*
8. Hayakawa, K., R. R. Hardy, M. Honda, L. A. Herzenberg, A. D. Steinberg, and L. A. Herzenberg. 1984. Ly-1 B cells: functionally distinct lymphocytes that secrete IgM autoantibodies. *Proc. Natl. Acad. Sci. USA 81:2494.*
9. Förster, I., and K. Rajewsky. 1987. Expansion and functional activity of Ly-1$^+$ B cells upon transfer of peritoneal cells into allotype-congenic newborn mice. *Eur. J. Immunol. 17:521.*
10. Haughton, F., L. W. Arnold, A. C. Whitmore, and S. H. Clarke. 1993. B-1 cells are made, not born. *Immunol. Today 14:84.*
11. Gay, D., T. Saunders, S. Camper, and M. Weigert. 1993. Receptor editing: an approach by autoreactive B cells to escape tolerance. *J. Exp. Med. 177:999.*
12. Tiegs, S. L., D. M. Russell, and D. Nemazee. 1993. Receptor editing in self-reactive bone marrow B cells. *J. Exp. Med. 177:1009.*
13. Chen, C., Z. Nagy, E. L. Prak, and M. Weigert. 1995. Immunoglobulin heavy chain gene replacement: a mechanism of receptor editing. *Immunity 3:747.*
14. Nemazee, D., D. Russell, B. Arnold, G. Haemmerling, J. Allison, J. F. A. P. Miller, G. Morahan, and K. Buerki. 1991. Clonal deletion of autospecific B lymphocytes. *Immunol. Rev. 122:117.*
15. Hartley, S. B., J. Crosbie, R. Brink, A. A. Kantor, A. Basten, and C. C. Goodnow. 1991. Elimination from peripheral lymphoid tissues of self-reactive B lymphocytes recognizing membrane-bound antigens. *Nature 353:765.*
16. von Boehmer, H. 1990. Developmental biology of T cells in T cell receptor transgenic mice. *Annu. Rev. Immunol. 8:531.*
17. Surh, C. D., and J. Sprent. 1994. T-cell apoptosis detected in situ during positive and negative selection in the thymus. *Nature 372:100.*
18. Tang, X., M. S. Halleck, R. A. Schlegel, and P. Williamson. 1996. A subfamily of P-type ATPases with aminophospholipid transporting activity. *Science 272: 1495.*
19. van Meer, G. 1993. Transport and sorting of membrane lipids. *Curr. Opin. Cell Biol. 5:661.*
20. Verhoven, B., R. A. Schlegel, and P. Williamson. 1995. Mechanisms of phosphatidylserine exposure, a phagocyte recognition signal, on apoptotic T lymphocytes. *J. Exp. Med. 182:1597.*
21. Fadok, V. A., D. L. Bratton, S. C. Frasch, M. L. Warner, and P. M. Henson. 1998. The role of phosphatidylserine in recognition of apoptotic cells by phagocytes. *Cell Death Differ. 5:551.*
22. Ren, Y., and J. Savill. 1998. Apoptosis: the importance of being eaten. *Cell Death Differ. 5:563.*
23. Gerke, V., and S. E. Moss. 1997. Annexins and membrane dynamics. *Biochim. Biophys. Acta 1357:129.*
24. van Engeland, M., L. J. W. Nieland, F. C. S. Ramaekers, B. Schutte, and C. P. M. Reutelingsperger. 1998. Annexin V-affinity assay: a review on an apoptosis detection system based on phosphatidylserine exposure. *Cytometry 31:1.*
25. Koopman, G., Reutelingsperger, C. P., Kuijten, G. A., Keehnen, R. M., Pals, S. T., and M. H. van Oers. 1994. Annexin V for flow cytometric detection of phosphatidylserine expression on B cells undergoing apoptosis. *Blood 84:1415.*
26. Russell, D. M., Z. Dembic, G. Morahan, J. F. Miller, K. Bürki, and D. Nemazee. 1991. Peripheral deletion of self-reactive B cells. *Nature 354:308.*
27. Koller, B. H., P. Marrack, J. W. Kappler, and O. Smithies. 1990. Normal development of mice deficient in β_2M, MHC class I proteins and CD8$^+$ T cells. *Science 248:1227.*
28. Goodnow, C., J. Crosbie, S. Adelstein, T. Lavoie, S. Smith-Gill, R. Brink, H. Pritchard-Briscoe, J. Wotherspoon, R. Loblay, K. Raphael, et al. 1988. Altered immunoglobulin expression and functional silencing of self-reactive B lymphocytes in transgenic mice. *Nature 334:676.*
29. Arnold, L. W., C. A. Pennell, S. K. McCray, and S. H. Clarke. 1994. Development of B-1 cells: segregation of phosphatidyl choline-specific B cells to the B-1 population occurs after immunoglobulin gene expression. *J. Exp. Med. 179:1585.*
30. Casciola-Rosen, L., A. Rosen, M. Petri, and M. Schlissel. 1996. Surface blebs on apoptotic cells are sites of enhanced procoagulant activity: implications for coagulation events and antigenic spread in systemic lupus erythematosus. *Proc. Natl. Acad. Sci. USA 93:1624.*
31. Casciola-Rosen, L. A., G. J. Anhalt, and A. Rosen. 1995. DNA-dependent protein kinase is one of a subset of autoantigens specifically cleaved early during apoptosis. *J. Exp. Med. 182:1625.*
32. Chen, Y.-Y., L. C. Wang, M. S. Huang, and N. Rosenberg. 1994. An active v-*abl* protein tyrosine kinase blocks immunoglobulin light chain gene rearrangement. *Genes Dev. 8:688.*
33. Martin, S. J., C. P. M. Reutelingsperger, A. J. McGahon, J. A. Rader, R. C. A. A. van Schie, D. M. LaFace, and D. R. Green. 1995. Early redistribution of plasma membrane phosphatidylserine is a general feature of apoptosis regardless of the initiating stimulus: inhibition by overexpression of Bcl-2 and Abl. *J. Exp. Med. 182:1545.*
34. Ozato, K., N. Mayer, and D. H. Sachs. 1980. Hybridoma cell lines secreting monoclonal antibodies to mouse H-2 and Ia antigens. *J. Immunol. 124:533.*
35. Lang, J., M. Jackson, L. Teyton, A. Brunmark, K. Kane, and D. Nemazee. 1996. B cells are exquisitely sensitive to central tolerance and receptor editing induced by ultralow affinity, membrane-bound antigen. *J. Exp. Med. 184:1685.*
36. Nemazee, D., and K. Bürki. 1989. Clonal deletion of B lymphocytes in a transgenic mouse bearing anti-MHC class I antibody genes. *Nature 337:562.*
37. Wyllie, A. H. 1980. Glucocorticoid-induced thymocyte apoptosis is associated with endogenous endonuclease activation. *Nature 284:555.*
38. Moore, A., C. J. Donahue, K. D. Bauer, and J. P. Mather. 1998. Simultaneous measurement of cell cycle and apoptotic cell death. *Methods Cell Biol. 57:265.*
39. Kroemer, G., N. Zamzami, and S. A. Susin. 1997. Mitochondrial control of apoptosis. *Immunol. Today 18:45.*

40. Zamzami, N., P. Marchetti, M. Castedo, C. Zanin, J. L. Vayssiere, P. X. Petit, and G. Kroemer. 1995. Reduction in mitochondrial potential constitutes an early irreversible step of programmed lymphocyte death in vivo. *J. Exp. Med. 181:1661.*
41. Williamson, P., K. Mattocks, and R. A. Schlegel. 1983. Merocyanine 540: a fluorescent probe sensitive to lipid packing. *Biochim. Biophys. Acta 732:387.*
42. Mower, D. A., D. W. Peckham, V. A. Illera, J. K. Fishbaugh, L. L. Stunz, and R. F. Ashman. 1994. Decreased membrane phospholipid packing and decreased cell size precede DNA cleavage in mature mouse B cell apoptosis. *J. Immunol. 152:4832.*
43. Nunez, G., M. A. Benedict, Y. Hu, and N. Inohara. 1998. Caspases: the proteases of the apoptotic pathway. *Oncogene 17:3237.*
44. Kaufmann, S. H., S. Desnoyers, Y. Ottaviano, N. E. Davidson, and G. G. Poirier. 1993. Specific proteolytic cleavage of poly(ADP-ribose) polymerase: an early marker of chemotherapy-induced apoptosis. *Cancer Res. 53:3976.*
45. Vanags, D. M., M. I. Porn-Ares, S. Coppola, D. H. Burgess, and S. Orrenius. 1996. Protease involvement in fodrin cleavage and phosphatidylserine exposure in apoptosis. *J. Biol. Chem. 271:31075.*
46. Braun, J., and E. Unanue. 1980. B lymphocyte biology studied with anti-Ig antibodies. *Immunol. Rev. 52:3.*
47. Jacobson, K., and C. Dietrich. 1999. Looking at lipid rafts? *Trends Cell Biol. 9:87.*
48. Varma, R., and S. Mayor. 1998. GPI-anchored proteins are organized in submicron domains at the cell surface. *Nature 394:798.*
49. Simons, K., and E. Ikonen. 1997. Functional rafts in cell membranes. *Nature 387:569.*
50. Schon, A., and E. Freire. 1989. Thermodynamics of intersubunit interactions in cholera toxin upon binding to the oligosaccharide portion of its cell surface receptor, ganglioside GM1. *Biochemistry 28:5019.*
51. Harder, T., P. Scheiffele, P. Verkade, and K. Simons. 1998. Lipid domain structure of the plasma membrane revealed by patching of membrane components. *J. Cell Biol. 141:929.*
52. Viola, A., S. Schroeder, Y. Sakakibara, and A. Lanzavecchia. 1999. T lymphocyte costimulation mediated by reorganization of membrane microdomains. *Science 283:680.*
53. Healy, J. I., R. E. Dolmetsch, R. S. Lewis, and C. C. Goodnow. 1998. Quantitative and qualitative control of antigen receptor signaling in tolerant B lymphocytes. *Novartis Found. Symp. 215:137.*
54. Healy, J. I., and C. C. Goodnow. 1998. Positive versus negative signaling by lymphocyte antigen receptors. *Annu. Rev. Immunol. 16:645.*
55. Savill, J. 1998. Phagocytic docking without shocking. *Nature 392:442.*
56. Dini, L., F. Autuori, A. Lentini, S. Oliverio, and M. Piacentini. 1992. The clearance of apoptotic cells in the liver is mediated by the asialoglycoprotein receptor. *FEBS Lett. 296:174.*
57. Schlegel, R. A., M. Callahan, S. Krahling, D. Pradhan, and P. Williamson. 1996. Mechanisms for recognition and phagocytosis of apoptotic lymphocytes by macrophages. *Adv. Exp. Med. Biol. 406:21.*
58. Buhl, A. M., and J. C. Cambier. 1997. Co-receptor and accessory regulation of B-cell antigen receptor signal transduction. *Immunol. Rev. 160:127.*
59. Fearon, D. T. 1998. The complement system and adaptive immunity. *Semin. Immunol. 10:355.*
60. Montixi, C., C. Langlet, A. M. Bernard, J. Thimonier, C. Dubois, M. A. Wurbel, J. P. Chauvin, M. Pierres, and H. T. He. 1998. Engagement of T cell receptor triggers its recruitment to low-density detergent-insoluble membrane domains. *EMBO J. 17:5334.*
61. Moran, M., and M. C. Miceli. 1998. Engagement of GPI-linked CD48 contributes to TCR signals and cytoskeletal reorganization: a role for lipid rafts in T cell activation. *Immunity 9:787.*
62. Wülfing, C., and M. M. Davis. 1998. A receptor/cytoskeletal movement triggered by costimulation during T cell activation. *Science 282:2266.*
63. Wülfing, C., M. D. Sjaastad, and M. M. Davis. 1998. Visualizing the dynamics of T cell activation: intracellular adhesion molecule 1 migrates rapidly to the T cell/B cell interface and acts to sustain calcium levels. *Proc. Natl. Acad. Sci. USA 95:6302.*
64. Xavier, R., T. Brennan, Q. Li, C. McCormack, and B. Seed. 1998. Membrane compartmentation is required for efficient T cell activation. *Immunity 8:723.*
65. Rodgers, W., and J. K. Rose. 1996. Exclusion of CD45 inhibits activity of $p56^{lck}$ associated with glycolipid-enriched membrane domains. *J. Cell Biol. 135:1515.*
66. Verhoven, B., S. Krahling, R. A. Schlegel, and P. Williamson. 1999. Regulation of phosphatidylserine exposure and phagocytosis of apoptotic T lymphocytes. *Cell Death Differ. 6:262.*
67. Brown, D. A., and E. London. 1998. Functions of lipid rafts in biological membranes. *Annu. Rev. Cell Dev. Biol. 14:111.*
68. Epand, R. M. 1998. Lipid polymorphism and protein-lipid interactions. *Biochim. Biophys. Acta 1376:353.*
69. Langner, M., and S. W. Hui. 1999. Merocyanine 540 as a fluorescence indicator for molecular packing stress at the onset of lamellar-hexagonal transition of phosphatidylethanolamine bilayers. *Biochim. Biophys. Acta 1415:323.*
70. Krop, I., A. L. Shaffer, D. T. Fearon, and M. S. Schlissel. 1996. The signaling activity of murine CD19 is regulated during B cell development. *J. Immunol. 157:48.*
71. Dolmetsch, R. E., R. S. Lewis, C. C. Goodnow, and J. I. Healy. 1997. Differential activation of transcription factors induced by Ca^{2+} response amplitude and duration. *Nature 386:855.*
72. Healy, J. I., R. E. Dolmetsch, L. A. Timmerman, J. G. Cyster, M. L. Thomas, G. R. Crabtree, R. S. Lewis, and C. C. Goodnow. 1997. Different nuclear signals are activated by the B cell receptor during positive versus negative signaling. *Immunity 6:419.*